STScI | SPACE TELESCOPE SCIENCE INSTITUTE

JWST TECHNICAL REPORT

Title: Improved NIRCam Flat Field Reference Files for Cycle 1	Doc #: JWST-STScI-008607, SM-12 Date: 30 November 2023 Rev: -
Authors: Ben Sunnquist, Martha Boyer, Brian Brooks, Alicia Canipe, Bryan Hilbert, Armin Rest Phone: 410-338-6807	Release Date: 16 February 2024

1 Abstract

Using a combination of commissioning and Cycle 1 GO data, we generate and deliver improved flat fields for all NIRCam imaging filters and detectors. These new flat fields correct remaining ~1-2% large-scale, filter-dependent gradients as well as pixel-level deviations upwards of ~10% in the longwave. The new longwave flat fields were delivered on May 3, 2023 (CRDS jwst_1083.pmap) and the new shortwave flat fields were delivered on September 12, 2023 (CRDS jwst_1125.pmap). Both sets of flat fields are now active by default in the JWST operational pipeline.

2 Introduction

Initial NIRCam flight data revealed large-scale ~6-8% flat variations from ground across all filters and detectors. As described in detail in Sunnquist et al. (2022), these deviations were corrected in a new batch of flat field reference files delivered shortly after commissioning (CRDS jwst_0953.pmap). While these corrections reduced the large-scale flat field deviations down to ~1-2%, the data available at the time was limited, and they did not provide filter or pixel-level corrections. In this paper, we incorporate the plethora of deep Cycle 1 GO data to generate updated skyflats to correct both the remaining filter-dependent, large-scale gradients in these flat fields as well as the strong pixel-level deviations in the longwave.

3 New Flat Field Reference Files

We follow a similar procedure used by NIRCam (Sunnquist et al., 2022) and WFC3/IR (Mack et al., 2021; Pirzkal et al., 2011) to improve the NIRCam flat field quality. In brief, we generate normalized, source-masked median stacks of all deep NIRCam data since commissioning for all detectors and filters. The resulting images, i.e. the delta skyflats, are then applied to the existing flat field reference files to correct these deviations by default in the JWST pipeline.

3.1 Data

To generate the skyflats, we consider all NIRCam full-frame data of sparse fields with ~uniform background illumination taken from March 23, 2022 to February 22, 2023. The start time corresponds to when JWST was fully cooled in commissioning, and there was no more MIRI thermal contamination in the NIRCam longwave channel. We avoid shorter (<300 second) exposures and only consider wide-band filters (with the exception of F070W), as we find that the narrow and medium-band skyflats did not have adequate SNR to improve the flat fields. We visually inspect each remaining image, and exclude any with extended objects (nebulas, large galaxies, etc.) as well as those with scattered light, persistence, or other anomalous issues. In total, our final skyflats incorporate between 505-1138 images from 40 unique programs. Depending on the detector and filter, we find this gives us total signals of ~50,000-100,000 electrons/pixel in the shortwave, and ~130,000-780,000 electrons/pixel in the longwave. Each image was calibrated using JWST pipeline v1.8.2 and CRDS context jwst_1041.pmap.

3.2 Generating the New Flat Field Reference Files

Using the data described in Section 3.1, we create delta skyflats for each filter and detector following a similar procedure used by NIRCam (Sunnquist et al., 2022) and WFC3/IR (Mack et al., 2021; Pirzkal et al., 2011). For each calibrated image (i.e. _cal.fits file), we first use photutils source detection to create a corresponding source mask; we smooth the image with a 3x3 pixel gaussian filter and flag any 6 interconnecting pixels 1 sigma above the background as a source. To ensure we flag the extent of larger sources, we expand the masks of extended sources (defined as those with 200 interconnected pixels) outwards by 30 pixels in all directions. We also include any pixels flagged as DO_NOT_USE in the data quality arrays in these masks. Next, we normalize each image by their source-masked, sigma-clipped median. The final delta skyflats are then the sigma-clipped median through the stack of all of these normalized, source-masked images. We use weighted sums of the wide-band delta skyflats to create the delta skyflats for the narrow and medium-band filters, as the latter did not have enough SNR for standalone corrections. We confirmed that this method was reasonable for F410M, which was one medium-band filter whose standalone delta skyflat had moderate SNR suitable for comparison.

3.2.1 Longwave Flat Fields

For the longwave delta skyflats, we ignore (i.e. set to 1) any pixels with values greater than 1.1 adjacent to DO_NOT_USE pixels, as it appeared these high outliers may be due to some other effect such as interpixel capacitance. We also ignore any pixels with values lower than 0.6 so long as they aren't part of a larger dead pixel concentration; we find that these standalone dead pixels generally don't correct real effects in test data, but rather imprint high outliers in the data after flat-fielding. After making these adjustments, we multiply these delta skyflats onto the existing flat field reference files, and deliver these new reference files to CRDS (jwst_1083.pmap) to correct these deviations by default in the JWST pipeline. Figure 1 shows the final delta skyflats for each longwave filter. In addition to large-scale, filter-dependent gradients of ~1-2%, we also see large pixel-level deviations in these delta skyflats upwards of ~10%, e.g. in the crosshatching regions.

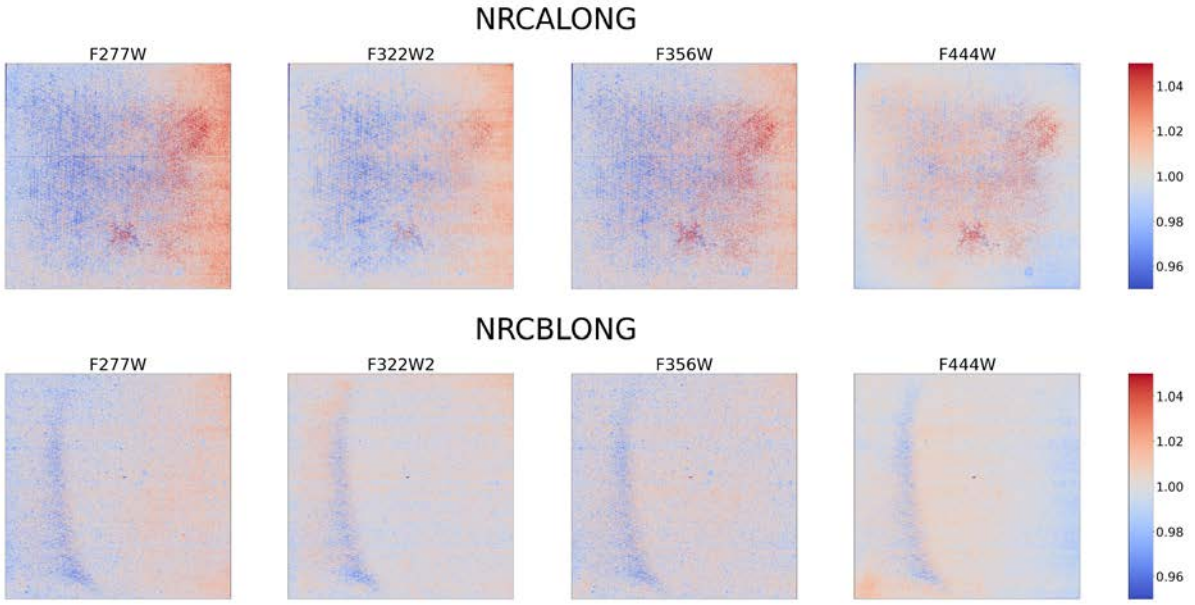

Figure 1: Delta skyflats for each longwave detector and filter.

In Figure 2, we show the improvement these new longwave flat field reference files give in dithered imaging data of the public CEERS program 1345 (Finkelstein et al., 2017). In this test case, we see both the large-scale gradients and strong pixel-level deviations are removed when using the new flat fields, resulting in a decrease in the background RMS of 22%.

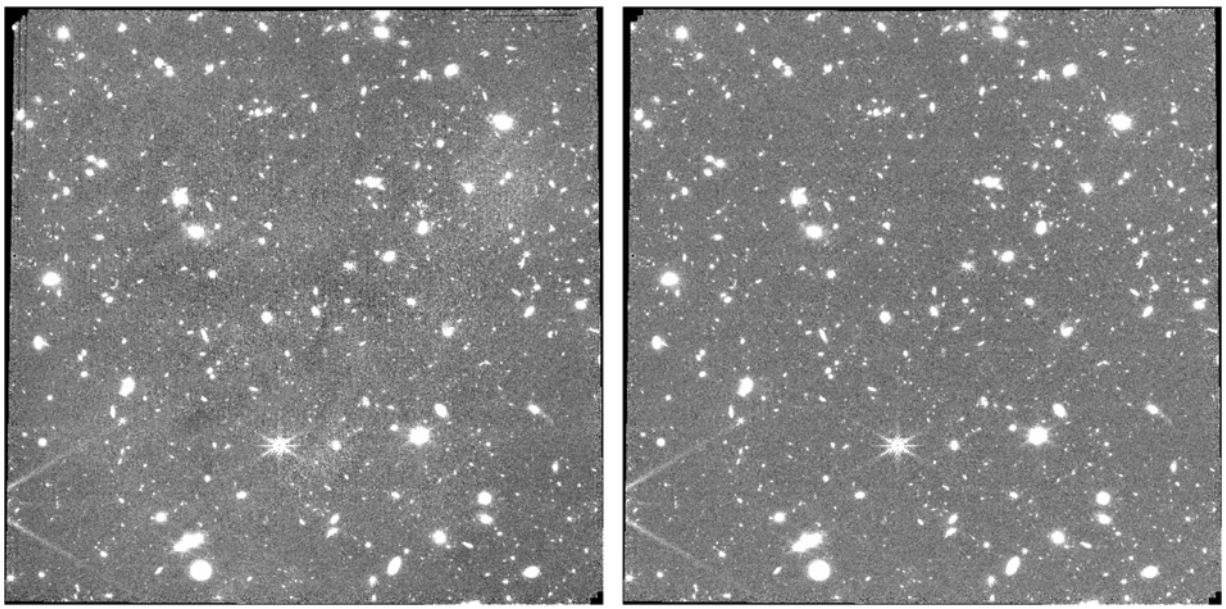

Figure 2: The improvement in drizzled image quality using the old (left) and new (right) longwave flat field reference files. The example here uses ALONG F444W images from PID-1345 observation 1.

3.2.2 Shortwave Flat Fields

We find that large portions of the shortwave delta skyflats are contaminated by both large-scale persistence and the scattered light wisps. Without a sufficient method to correct these features, we first opt to mask these regions in the delta skyflats and replace them with a 2nd order 2D polynomial fit performed on the remaining, unmasked pixels. In our delta skyflats, persistence mainly affects the left edges of detectors A3 and B4, the bottom left corner of B2, and the top right corner of B3, which corresponds to those regions identified in Leisenring et al. (2016) as most susceptible to persistence. The source of persistence in the individual images varies and includes nebulas, stellar clusters, planets, and even high background observations; however, in some cases the cause of persistence is unknown, and may result while the telescope is slewing as NIRCam is fully exposed to bright objects across its FOV during this time. Wisps affect the top central portions of detectors A3 and B4, and the bottom central portions of A4 and B3, especially in redder wavelengths (Sunnquist et al., 2022). Figure 3 highlights these regions in the F115W delta skyflats before any masking and smoothing occurred.

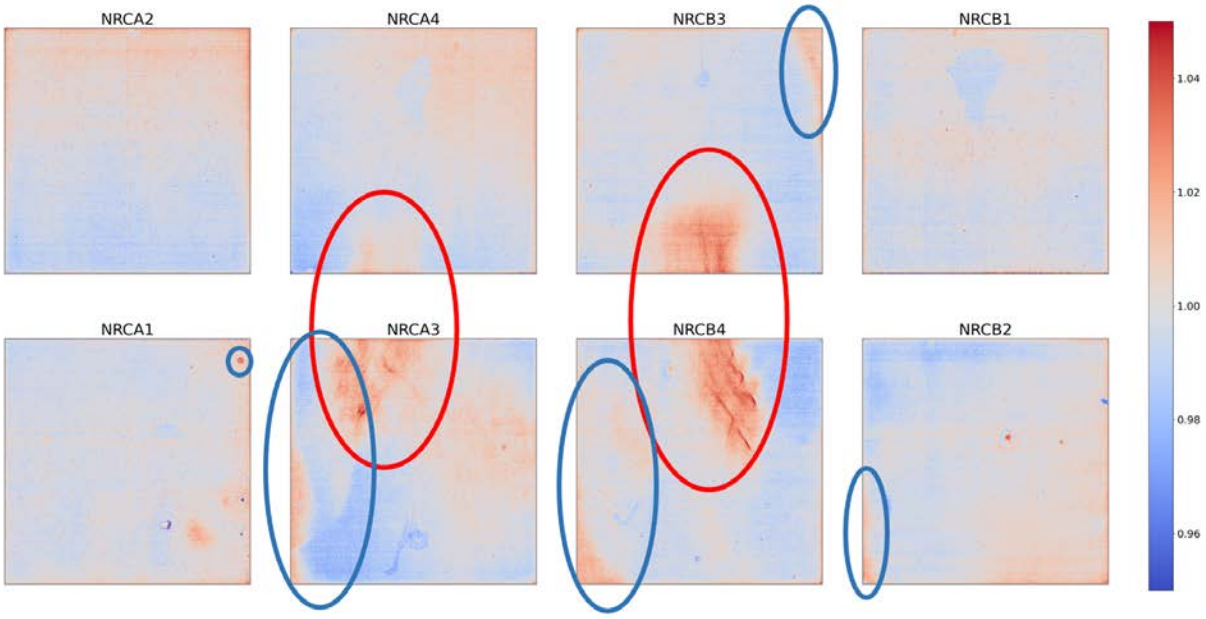

Figure 3: F115W delta skyflats showing areas contaminated by scattered light wisps (red circles) and large-scale persistence (blue circles).

Due to these large-scale contamination issues, as well as the lower total signal and lack of strong pixel-level deviations compared to the longwave, we opt to further smooth the shortwave delta skyflats using a 2D median filter (8x8 pixel filter on top of a 32x32 pixel low resolution filter). We then multiply these smoothed delta skyflats onto the existing flat field references files, and deliver these new reference files to CRDS (jwst_1125.pmap) to correct these deviations by default in the JWST pipeline. Figure 4 shows the final delta skyflats for each shortwave filter. As seen in Figure 4, the shortwave corrections are generally larger-scale, filter-dependent gradients at a level of ~1-2%. Notably, the low epoxy regions (Hilbert & Rest, 2016) at the top centers of A4 and B1 are ~1-2% lower than surrounding pixels in these delta skyflats as well.

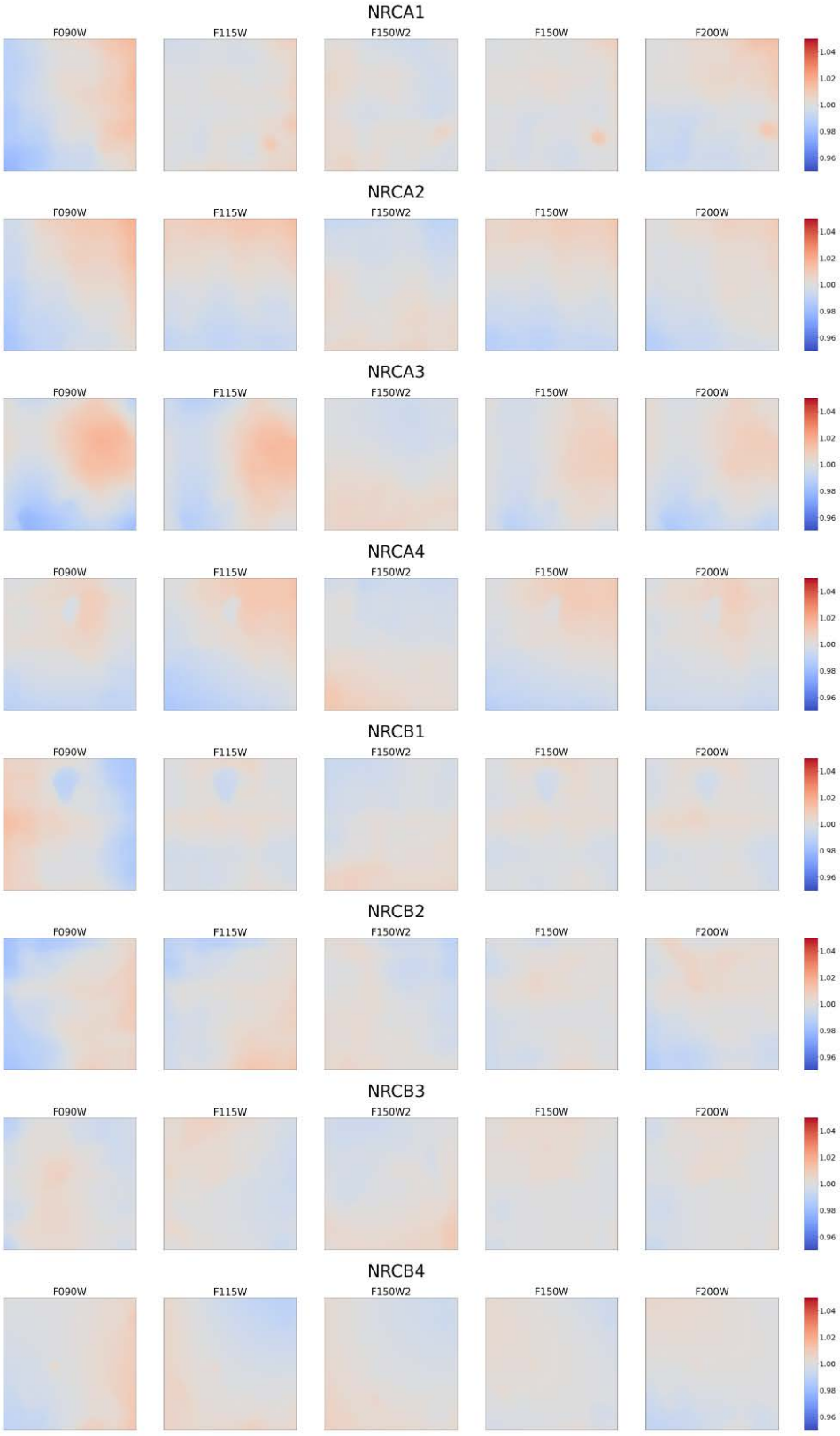

Figure 4: Delta skyflats for each shortwave detector and filter.

In Figure 5, we show the improvement these new shortwave flat field reference files give in dithered imaging data of the NGDEEP program 2079 (Finkelstein et al., 2021). In this test case, we see the large-scale ~2% top-down gradient characteristic of A2 F150W (see Figure 4) is removed.

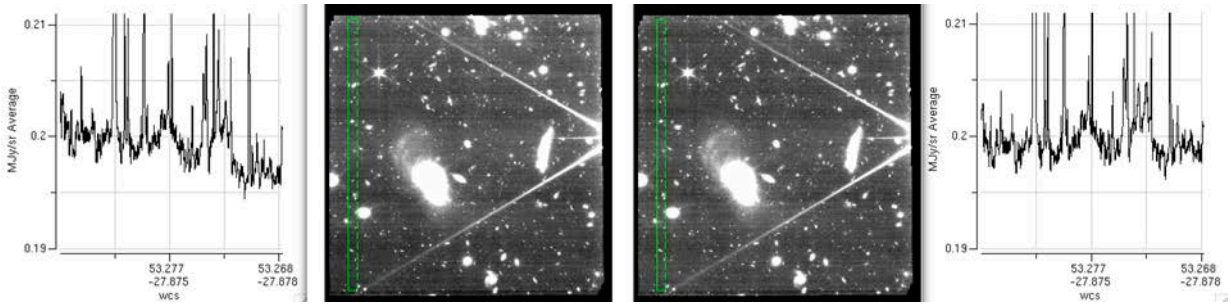

Figure 5: The improvement in drizzled image quality using the old (left) and new (right) shortwave flat field reference files, as well as their median-collapsed row values through a slice of the image. The example here uses A2 F150W images from PID-2079 observation 4.

4 Conclusions

Using the large amount of NIRCam imaging data observed throughout Cycle 1 and commissioning, we generated and delivered improved NIRCam flat field reference files for all imaging filters and detectors to CRDS (jwst_1083.pmap for longwave; jwst_1125.pmap for shortwave). These new reference files correct remaining ~1-2% large-scale, filter-dependent gradients as well as strong pixel-level deviations upwards of ~10% in the longwave.

5 References

Finkelstein, S. L., Dickinson, M., Ferguson, H. C., et al., 2017, JWST Proposal ID 1345, Cycle 1 ERS

Finkelstein, S. L., Papovich, C., Pirzkal, N., et al., 2021, JWST Proposal ID 2079, Cycle 1 GO

Hilbert, B., and Rest, A., 2016, Technical Report JWST-STScI-004622, "NIRCam Detector Gain Values in CV2"

Leisenring, J., Rieke, M., Misselt, K., and Robberto, M., 2016, Proc. SPIE 9915, "Characterizing persistence in JWST NIRCam flight detectors"

Mack, J., Olszewksi, H., and Pirzkal, N., 2021, WFC3 ISR 2021-01, "WFC3/IR Filter-Dependent Sky Flats"

Pirzkal, N., Mack, J., Dahlen, T., et al., 2011, WFC3 ISR 2011-11, "Sky Flats: Generating Improved WFC3 IR Flat-fields"

Sunnquist, B., Willmer, C., Brooks, B., et al., 2022, Technical Report JWST-STScI-008304, "NIRCam Commissioning Results NRC-10: Flat Fields, Scattered Light, and Backgrounds"